J. Phase Equilib. Diffus. (2019) 40:508–521
https://doi.org/10.1007/s11669-019-00736-w

Multiscale Entropy and Its Implications to Critical Phenomena, Emergent Behaviors, and Information

Zi-Kui Liu[1] · Bing Li[2] · Henry Lin[3]

Submitted: 16 January 2019 / in revised form: 28 May 2019 / Published online: 18 June 2019

Abstract Thermodynamics of critical phenomena in a system is well understood in terms of the divergence of molar quantities with respect to potentials. However, the prediction and the microscopic mechanisms of critical points and the associated property anomaly remain elusive. It is shown that while the critical point is typically considered to represent the limit of stability of a system when the system is approached from a homogenous state to the critical point, it can also be considered to represent the convergence of several homogeneous subsystems to become a macro-homogeneous system when the critical point is approached from a macro-heterogeneous system. Through the understanding of statistic characteristics of entropy in different scales, it is demonstrated that the statistic competition of key representative configurations results in the divergence of molar quantities when metastable configurations have higher entropy than the stable configuration. Furthermore, the connection between change of configurations and the change of information is discussed, which provides a quantitative framework to study complex, dissipative systems.

Keywords critical phenomena · entropy · information · invar · perovskites · second law of thermodynamics · statistic thermodynamics

1 Introduction

Thermodynamics is a science concerning the state of a system described by a set of state variables. Entropy is one of the state variables, representing the degree of disorder of the system, i.e., the higher the disorder, the larger the entropy.[1] While the first law of thermodynamics is on the energy conservation, the second law of thermodynamics dictates that any internal process (IP or ip) in a system must produce entropy if it proceeds spontaneously and irreversibly. It should be noted though that the total entropy change of the system also depends on how the system exchanges entropy with the surroundings through heat and mass and can be either positive or negative, and it is the combined first and second laws of thermodynamics that represents the over-all progress of the system. The degree of order or disorder of a system may thus either increase or decrease based on the external conditions and internal processes, resulting in the change of the state of the system in terms of internal configurations and their probabilities that are denoted by the configurational entropy at the corresponding time and space scales.

Each of those configurations can be considered as a subsystem itself with its own set of sub-configurations. For

This article is an invited paper selected from presentations at "PSDK XIII: Phase Stability and Diffusion Kinetics," held during MS&T'18, October 14-18, 2018, in Columbus, Ohio. The special sessions were dedicated to honor Dr. John Morral, recipient of the ASM International 2018 J. Willard Gibbs Phase Equilibria Award "for fundamental and applied research on topology of phase diagrams and theory of phase equilibria resulting in major advances in the calculation and interpretation of phase equilibria and diffusion." It has been expanded from the original presentation.

✉ Zi-Kui Liu
prof.zikui.liu@psu.edu

[1] Department of Materials Science and Engineering, The Pennsylvania State University, University Park, PA 16802

[2] Department of Statistics, The Pennsylvania State University, University Park, PA 16802

[3] Department of Ecosystem Science and Management, The Pennsylvania State University, University Park, PA 16802

example, one can investigate the entropy of the universe and a black hole,[2,3] a society,[4,5] an ecosystem,[6] a person[7] or a compound,[8] and the entropy from the smaller scale is homogenized and contributes to the entropy at the larger scale. The present paper aims to discuss how the homogenization of configurations can be formulated and exchanged between scales in terms of configurational entropies at different scales, its probability at neighboring scale and its application to systems with critical points. Additionally, the entropy production of an internal process is correlated with the generation and erasure of information and reflects the information stored in the system in terms of multiscale configurations. It is noted that the present work is closely related to the renormalization theories[9,10] with the system at one scale consisting of self-similar copies of itself when viewed at another scale, and the different parameters at various scales are used to describe the constituents of the system. It is shown in the present work that the entropy and statistical probability of each configuration are the parameters that connect the scales.

2 Review of Fundamentals of Entropy

In thermodynamics, the entropy change of a system, dS, can be written as follows[11,12]

$$dS = \frac{dQ}{T} + \sum S_i dN_i + d_{\mathrm{ip}}S \qquad \text{(Eq 1)}$$

where dQ and dN_i are the heat and the amount of component i that the system receives from or release to the surroundings, T is the temperature, S_i is the molar entropy of component i in the surroundings for $dN_i > 0$ or the system for $dN_i < 0$, often called partial entropy of component i, and $d_{\mathrm{ip}}S$ is the entropy production due to independent IPs with each that may contain a group of coupled processes. It is evident that the first two terms concern the interactions between the surroundings and the system, while the third term embodies what happens inside the system. Equation 1 thus establishes a bridge connecting the interior of a system in terms of internal entropy production and the exterior of the system in terms mass and heat exchanges.

Combining Eq 1 with the first law of thermodynamics, the combined law of thermodynamics can be obtained. While the work exchanges between the system and surrounding can involve mechanical, electric, and magnetic works, it is often that the work due to hydrostatic pressure is considered,[11,12] and the combined law of thermodynamics is written as follows

$$\begin{aligned} dU &= TdS - PdV + \sum \mu_i dN_i - Td_{\mathrm{ip}}S \\ &= \sum Y^a dX^a - Td_{\mathrm{ip}}S \end{aligned} \qquad \text{(Eq 2)}$$

where T, P and V are temperature, pressure, and volume, respectively, and μ_i is the chemical potential of component i. In the second part of Eq 2, Y^a denotes the potentials, i.e., T, $-P$ and μ_i, and X^a denotes the molar quantities, i.e., S, V and N_i.[11,12] It should be emphasized that both dV and dN_i in Eq 2 refer to the changes between the system and surroundings, while dS contains the contributions from IPs as shown by Eq 1.

By introducing the driving force for each independent IP, j, the energy change due to the entropy production can be represented by the product of driving force for the IP, $D_{\mathrm{ip},j}$, and the change of corresponding internal variable, $d\xi_j$, in terms of the Taylor expansion up to the third order as follows[11]

$$\begin{aligned} Td_{\mathrm{ip}}S = &\sum D_{\mathrm{ip},j} d\xi_j - \frac{1}{2}\sum D_{\mathrm{ip},jk} d\xi_j d\xi_k \\ &+ \frac{1}{6}\sum D_{\mathrm{ip},jkl} d\xi_j d\xi_k d\xi_l \end{aligned} \qquad \text{(Eq 3)}$$

where the second and third terms are added for discussion of stability of the system based on their signs when the first summation in the equation equals zero, i.e. the system is at a state of equilibrium.[13]

The second law of thermodynamics requires that each independent IP, if proceeding spontaneously, must have a positive entropy production, i.e. $D_{\mathrm{ip},j} > 0$ to give $Td_{\mathrm{ip}}S > 0$. Consequently, the system reaches a state of equilibrium when $D_{\mathrm{ip},j} \le 0$ for all IPs. This equilibrium state is stable with respect to fluctuations of internal variables when $D_{\mathrm{ip},jk} > 0$ due to the negative entropy production and unstable when $D_{\mathrm{ip},jk} < 0$ due to the positive entropy production for the IP of interest, both as shown by Eq 3. When $D_{\mathrm{ip},jk} = 0$ the system is at the limit of stability. The limit of stability becomes a critical point in the space of independent internal variables $\xi_j \xi_k \xi_l$ with additional $D_{\mathrm{ip},jkl} = 0$. The critical point in the space of all possible independent internal variables of the system is termed as the invariant critical point (ICP).[14] For a homogeneous system, the IPs involve the movement of molar quantities inside the system, and one can write the stability variables of one IP as follows[11]

$$D_{\mathrm{ip},X^aX^a} = \left[\frac{\partial^2 U}{\partial (X^a)^2}\right]_{X^b} = \left[\frac{\partial Y^a}{\partial X^a}\right]_{X^b} \qquad \text{(Eq 4)}$$

$$D_{\mathrm{ip},X^aX^aX^a} = \left[\frac{\partial^3 U}{\partial (X^a)^3}\right]_{X^b} = \left[\frac{\partial^2 Y^a}{\partial (X^a)^2}\right]_{X^b} \qquad \text{(Eq 5)}$$

For heterogeneous systems with chemical reactions, the IPs are more complicated and may or may not be explicitly spelled out.[15]

Equation 1 concerns the change of entropy. To obtain the absolute value of entropy, one can integrate the

equation under the condition of reversible addition of heat to the system in equilibrium with $dN_i = 0$ and $d_{ip}S = 0$, i.e.

$$S = S_0 + \int_0^T \frac{CdT}{T} \quad \text{(Eq 6)}$$

where S_0 is the entropy at zero Kelvin, conventionally assigned to be zero in terms of the third law of thermodynamics, and C the heat capacity of the system, denoting the heat needed to increase the temperature of the system by one degree.

3 Statistics of Entropy

The discussion in the previous section has not concerned the statistic characteristics of entropy. Gibbs[16] pointed out that the entropy is defined as the average value of the logarithm of probability of phase where the differences in phases are with respect to configuration. Therefore, the configurational entropy in a system of interest with properly defined time and space scales can be written as

$$S^{\text{conf}} = -k_B \sum_{k=1}^{m} p^k \ln p^k \quad \text{(Eq 7)}$$

where k_B is the Boltzmann constant, and p^k the probability of configuration $k \in \{1, \ldots, m\}$ of the system with $\sum_{k=1}^{m} p^k = 1$ as shown in the upper row of Fig. 1(a). Since each configuration k has its own entropy, S^k, the total entropy of the system can be written as

$$S = \sum_{k=1}^{m} p^k S^k + S^{\text{conf}} = \sum_{k=1}^{m} p^k \left(S^k - k_B \ln p^k\right) \quad \text{(Eq 8)}$$

Equations 6 and 8 should give the same entropy value when they are counted on the same time and space scales.

By the same token, the configuration k is composed of configurations in the scale of short time and smaller dimension and can be written as

$$S^k = \sum_{l=1}^{n} p^{l|k} \left(S^{l|k} - k_B \ln p^{l|k}\right) \quad \text{(Eq 9)}$$

where $p^{l|k}$ and $S^{l|k}$ are the conditional probability and entropy of configuration $l \in \{1, \ldots, n\}$ as sub-configurations of configuration k with $\sum_{l=1}^{n} p^{l|k} = 1$ as shown in the lower row of Fig. 1(a). Equation 8 can then be re-organized as follows

$$S = \sum_{k=1}^{m} p^k \left(\sum_{l=1}^{n} p^{l|k} \left(S^{l|k} - k_B \ln p^{l|k}\right) - k_B \ln p^k \right) \quad \text{(Eq 10)}$$

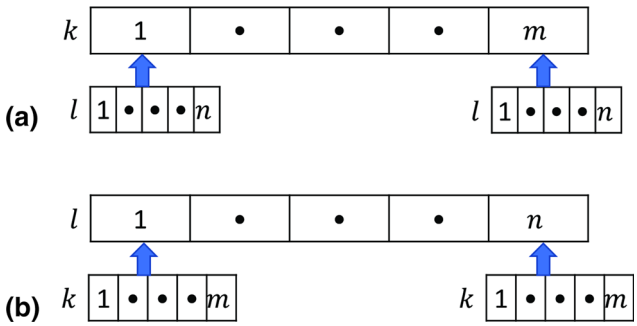

Fig. 1 Two scenarios of configurations of a system, (a) $k \in \{1, \ldots, m\}$ configurations with each of them composed of $l \in \{1, \ldots, n\}$ sub-configurations; (b) $l \in \{1, \ldots, n\}$ configurations with each being the statistic average of each $l \in \{1, \ldots, n\}$ sub-configuration in all $k \in \{1, \ldots, m\}$ configurations

This equation can be extended in the directions of larger and smaller dimensions to capture more complexity of the system or in the directions of longer and shorter time to capture evolution of the system. The examples of configurations $k \in \{1, \ldots, m\}$ and $l \in \{1, \ldots, n\}$ are the magnetic spin and vibrational configurations for cerium and Fe_3Pt, and the atomic and vibrational configurations for the miscibility gap in the fcc Al-Zn solution, respectively, discussed in section 6.

On the other hand, from a statistics point of view, one can calculate the direct contributions from the configurations in the scale l to the system as follows by re-organizing Eq 10 with the joint probability defined as $p^{k,l} = p^k p^{l|k}$,

$$\begin{aligned} S &= \sum_{k=1}^{m} \sum_{l=1}^{n} p^k p^{l|k} \left(S^{l|k} - k_B \ln\left(p^k p^{l|k}\right)\right) \\ &= \sum_{k=1}^{m} \sum_{l=1}^{n} p^{k,l} \left(S^{l|k} - k_B \ln p^{k,l}\right) \end{aligned} \quad \text{(Eq 11)}$$

It is self-evident that Eq 11 is the same as the combination of Eq 8 and 9 due to $\sum_{l=1}^{n} p^{l|k} = 1$ and $\sum_{l=1}^{n} \left(p^{l|k} k_B \ln p^k\right) = k_B \ln p^k$. Furthermore, one may attempt to switch the order of summation of k and l, i.e.,

$$S = \sum_{l=1}^{n} \left[\left(\sum_{k=1}^{m} p^{k,l} S^{l|k} \right) - k_B \sum_{k=1}^{m} p^{k,l} \ln p^{k,l} \right] \quad \text{(Eq 12)}$$

This is analogue to Eq 10, but with the configuration $l \in \{1, \ldots, n\}$ with sub-configuration of $k \in \{1, \ldots, m\}$ as shown in Fig. 1(b). As proved below, the two scenarios in Fig. 1(a) and (b) indeed give the same entropy of the system.

Let us define the following

$$q^l = \sum_{k=1}^{m} p^k p^{l|k} \quad \text{(Eq 13)}$$

$$q^{k|l} = \frac{p^k p^{l|k}}{\sum_{k=1}^{m} p^k p^{l|k}} = \frac{p^k p^{l|k}}{q^l} = \frac{p^{k,l}}{q^l} \quad \text{(Eq 14)}$$

$$T^l = \sum_{k=1}^{m} q^{k|l}\left(S^{l|k} - k_B \ln q^{k|l}\right) \quad \text{(Eq 15)}$$

where $\sum_{l=1}^{n} q^l = 1$, $\sum_{k=1}^{m} q^{k|l} = 1$, T^l is the entropy of a configuration in $l \in \{1, \ldots, n\}$ with sub-configuration of $k \in \{1, \ldots, m\}$ (see Fig. 1b), and Eq 14 the commonly referred Bayes's theorem.[17] It can be seen that T^l consists of two parts: a) the entropy of each configuration in the lower row of Fig. 1(b), i.e. $\sum_{k=1}^{m} q^{k|l} S^{l|k}$ which is evaluated from the entropy of each configuration in $l \in \{1, \ldots, n\}$ for all configurations in $k \in \{1, \ldots, m\}$, and b) the configuration among them, i.e. $-k_B \sum_{k=1}^{m} q^{k|l} \ln q^{k|l}$.

The proof for the fact that the two scenarios schematically depicted in Fig. 1(a) and (b) have the same entropy is as follows.

Theorem *If*

$$S = \sum_{k=1}^{m} p^k \left(S^k - k_B \ln p^k\right) \quad \text{(Eq 16)}$$

then

$$S = \sum_{l=1}^{n} q^l \left(T^l - k_B \ln q^l\right) \quad \text{(Eq 17)}$$

Proof From Eq 11 or 12 and using Eq 13 to 15

$$\begin{aligned} S &= \sum_{l=1}^{n}\sum_{k=1}^{m} p^{k,l}\left(S^{l|k} - k_B \ln p^{k,l}\right) \\ &= \sum_{l=1}^{n}\sum_{k=1}^{m} q^l q^{k|l}\left(S^{l|k} - k_B \ln q^l q^{k|l}\right) \\ &= \sum_{l=1}^{n} q^l \left\{\sum_{k=1}^{m} q^{k|l}\left(S^{l|k} - k_B \ln q^l q^{k|l}\right)\right\} \\ &= \sum_{l=1}^{n} q^l \left\{\left[\sum_{k=1}^{m} q^{k|l}\left(S^{l|k} - k_B \ln q^{k|l}\right)\right] - k_B \ln q^l \sum_{k=1}^{m} q^{k|l}\right\} \\ &= \sum_{l=1}^{n} q^l \left(T^l - k_B \ln q^l\right) \end{aligned} \quad \text{(Eq 18)}$$

This proof is important as it demonstrates that the sequence of configuration averaging can be switched in terms of their scales, i.e. either at the scale $k \in \{1, \ldots, m\}$ or $l \in \{1, \ldots, n\}$ with the other scale as its sub-configurations as schematically depicted in Fig. 1(a) and (b). Provided individual and joint probabilities of configurations in the system can be evaluated, the entropy of the system remains invariant independent of the scale where the statistic averaging is carried out. The implications of this conclusion will be further discussed in section 6.

4 Probability of Configurations

Probability of individual configurations of a system at given time and space scales can be evaluated when their energetics are known at the corresponding time and space scales through their partition functions. For a closed system under constant temperature and volume, a collection of possible configurations of the system comprises a canonical ensemble. In the discrete form, the canonical partition function is defined as follows[18]

$$Z = \sum_k Z^k = \sum_k e^{-\frac{F^k}{k_B T}} \quad \text{(Eq 19)}$$

where Z^k and F^k are the partition function and Helmholtz energy of configuration k with

$$F^k = -k_B T \ln Z^k \quad \text{(Eq 20)}$$

It should be mentioned that in the literature, the internal or total energy, U^k, is often used in the place of F^k, which implicitly assumes that the entropy of each configuration is negligible. This assumption is not valid at high temperatures as the individual configurations can have different entropy values resulting in significant change of their respective probabilities. It is noted that Asta et al.[19] used an equation similar to Eq 19 for systems under constant temperature, pressure, and chemical potentials.

The probability of each configuration can be defined as

$$p^k = \frac{Z^k}{Z} = e^{\frac{F - F^k}{k_B T}} \quad \text{(Eq 21)}$$

where F is the Helmholtz energy of the system and can be written as follows[8,20]

$$F = -k_B T \ln Z = \sum_k p^k F^k + k_B T \sum_k p^k \ln p^k \quad \text{(Eq 22)}$$

It can be seen that the configurational entropy by Eq 7 is shown in the last term in Eq 22, and from Eq 21 that $F \le F^k$ for $p^k \le 1$, originated from $\sum_k p^k \ln p^k \le 0$. The equality holds when the system has only one configuration.

The above discussion does not consider interactions between configurations. However, when the fluctuation dimension is smaller than the dimension of the system, there are interactions between configurations that may result in new configurations that are not part of the existing configurations. These interactions may be considered explicitly by adding interaction terms in Eq 22 similar to the CALPHAD modeling method in thermodynamics in the form of $p^j p^k L^{jk}$ with L^{jk} being the interaction

energy.[11,21,22] On the other hand, a better approach is to expand the set of configurations to include the new configurations with the statistic approach intact as discussed in this paper.

Furthermore, experimental measurements can only detect the combined effect from all configurations. For the properties of individual configurations, one has to rely on theoretic calculations. The first-principles quantum mechanics technique based on the density functional theory (DFT)[23] along with the sophisticated computer programs[24,25] and ubiquitous high performance computers[26,27] have enabled the quantitative predictions of ground states of a vast configurations as reflected in a number of online databases.[28–30] The Helmholtz energy of a configuration can be effectively evaluated from either phonon calculations[31,32] or the Debye model[33] with the scaling factor obtained from the elastic properties[34] predicted from first-principles calculations.[35–37] For configurations with disordering, the cluster expansion approach[38,39] or the special quasirandom structures (SQS)[40–42] can be used. It is also possible to sample configurations at finite temperatures through the ab initio molecular dynamics (AIMD) calculations[43] with the atomic forces computed on the fly using the DFT-based first-principles calculations as recently demonstrated for $PbTiO_3$ that are discussed in more detail in section 7.[44,45]

5 Thermodynamics of Critical Phenomena

Thermodynamics of critical phenomena is usually discussed in terms of the instability of a homogeneous system derived from the combined law, i.e. Eq 2, as Eq 4 and follows[11]

$$\frac{\partial Y^a}{\partial X^a} = 0 \qquad \text{(Eq 23)}$$

The thermodynamic criterion of instability based on entropy is written as

$$\frac{\partial T}{\partial S} = 0 \qquad \text{(Eq 24)}$$

When the system approaches the limit of stability,[11] this derivative approaches zero, and its inverse, i.e., the change of the entropy of the system, diverges, i.e.

$$\frac{\partial S}{\partial T} = +\infty \qquad \text{(Eq 25)}$$

The fluctuation of configurations reaches the whole system. After crossing the limit of stability, the system becomes inhomogeneous in the time and space scales under consideration.

Differentiation of Eq 8 with respect to temperature gives

$$\begin{aligned}\frac{\partial S}{\partial T} &= \sum_k \left[\frac{\partial p^k}{\partial T}\left(S^k - k_B \ln p^k\right) + p^k\left(\frac{\partial S^k}{\partial T} - \frac{k_B}{p^k}\frac{\partial p^k}{\partial T}\right)\right] \\ &= \frac{\partial S^N}{\partial T} \\ &\quad + \sum_{k\neq N}\left[\frac{\partial p^k}{\partial T}\left(S^k - S^N - k_B \ln \frac{p^k}{p^N}\right) + p^k\left(\frac{\partial S^k}{\partial T} - \frac{\partial S^N}{\partial T}\right)\right]\end{aligned} \qquad \text{(Eq 26)}$$

where N denotes the configuration with the lowest Helmholtz energy, i.e., the ground state at zero Kelvin, and $\sum_k p^k = 1$ and $\sum_k \frac{\partial p^k}{\partial T} = 0$ are used. In Eq 26, $\frac{\partial S^N}{\partial T}$ is positive from Eq 4, and the summation in Eq 26 would also be positive if $S^k > S^N$ that results in the increase of p^k from zero at zero Kelvin at the expense of p^N.

Differentiation of Eq 21 yields

$$\begin{aligned}\frac{\partial p^k}{\partial T} &= \frac{p^k}{k_B T^2}\left[\left(F^k - F\right) + T\left(S^k - S\right)\right] \\ &= \frac{p^k\left(S^k - S\right)}{k_B T}\left[1 + \frac{F^k - F}{T(S^k - S)}\right]\end{aligned} \qquad \text{(Eq 27)}$$

Equation 27 further demonstrates that $\frac{\partial p^k}{\partial T} > 0$ due to $S^k > S$ with $S \approx S^N$ at the limit of p^k near zero and $F^k > F$. It is evident that a dramatic increase of $\frac{\partial S}{\partial T}$ has to come from the dramatic increase of $\frac{\partial p^k}{\partial T}$, i.e., the significant competition between the metastable configurations $(k = 1 \ldots N-1)$ and the ground state configuration (N) with $F^k > F^N$. This means rapid change rate of some $\frac{F-F^k}{k_B T}$ in some temperature ranges with respect to the limit of stability.

Therefore, the thermodynamic criterion for instability and critical phenomena is that the entropies of metastable configurations are higher than that of the stable configuration, but their differences are large enough that the stable configuration remains stable with respect to the metastable configurations so that there are no first-order transitions until the instability and critical point are reached.

6 Examples: Anti-Invar Cerium, Invar Fe_3Pt, and Al-Zn binary

Cerium (Ce) is a unique element. Its ground state configuration under ambient pressure is non-magnetic face centered cubic (fcc) and its stable configuration at room temperature is ferromagnetic fcc with some degree of magnetic disordering, while all other magnetic elements in the chemical periodic table are opposite with their ground state configuration being magnetic. Ce has a critical point around T_C = 480-600 K and P_C = 1.45-2 GPa with the upper bound commonly accepted in the literature with details discussed in Ref. 46.

In an effort to predict the thermodynamic properties of Ce, we first considered two configurations: non-magnetic (NM) and ferromagnetic (FM) with their Helmholtz energies predicted by first-principles calculations using the partition function approach discussed above.[46] It should be noted that the entropy in the Helmholtz energy of each individual configuration contains the configurational contributions from lower scales, i.e. thermal electronic configurational contributions due to non-zero electronic density at the Fermi level and the vibrational frequency configurational contributions due to atomic vibrations as shown below[32]

$$F^k = E_c + F_{\text{vib}} + F_{\text{el}} \qquad \text{(Eq 28)}$$

where E_c is the static total energy at 0 K predicted by first-principles calculations, F_{vib} the lattice vibrational free energy, and F_{el} the thermal electronic contribution. The first term can be calculated directly using e.g. VASP code.[47] F_{vib} and F_{el} are related to contributions at finite temperatures with the same equation form as Eq 7. F_{el}, which is evaluated from the electronic densities of state at different volumes,[32] is important for metals due to the non-zero electronic density at the Fermi level. F_{vib} can be obtained from first-principles phonon calculations for accurate results[32,33] or the Debye model for the sake of simplicity using the modified scaling factor.[34]

However, the consideration of two configurations was not able to reproduce the experimentally observed critical phenomena. This is because their fluctuations in the finite space result in the interactions of magnetic spins in different orientations which are not captured by the two configurations considered. Following the conventional approach in the literature, an additional contribution to the free energy of the system in terms of 'local-moment' mechanism was added to account for the magnetic spin disordering, resulting in good agreement with experimental observations as shown in Fig. 2 for total entropy and T–V phase diagram along with all other anomalies in the system as detailed in Ref. 46 such as the critical point at $T_C = 476\,\text{K}$ and $P_C = 2.22\,\text{GPa}$.

The next step is to add an antiferromagnetic (AFM) configuration. The first-principles calculations predict that the static energy of the AFM configuration is between those of NM and FM configurations.[48] Since the interaction due to magnetic spin disordering is included in the AFM configuration, the 'local-moment' mechanism was no-longer needed. The fluctuation of the NM, AFM, and FM configurations enabled the predictions of all anomalies in the system as shown in Fig. 3 for various entropy changes and T-P phase diagram in addition to Schottky anomaly for heat capacity. Particularly the overestimated entropy change of the transition along the phase boundary in our previous work with two configurations only and the

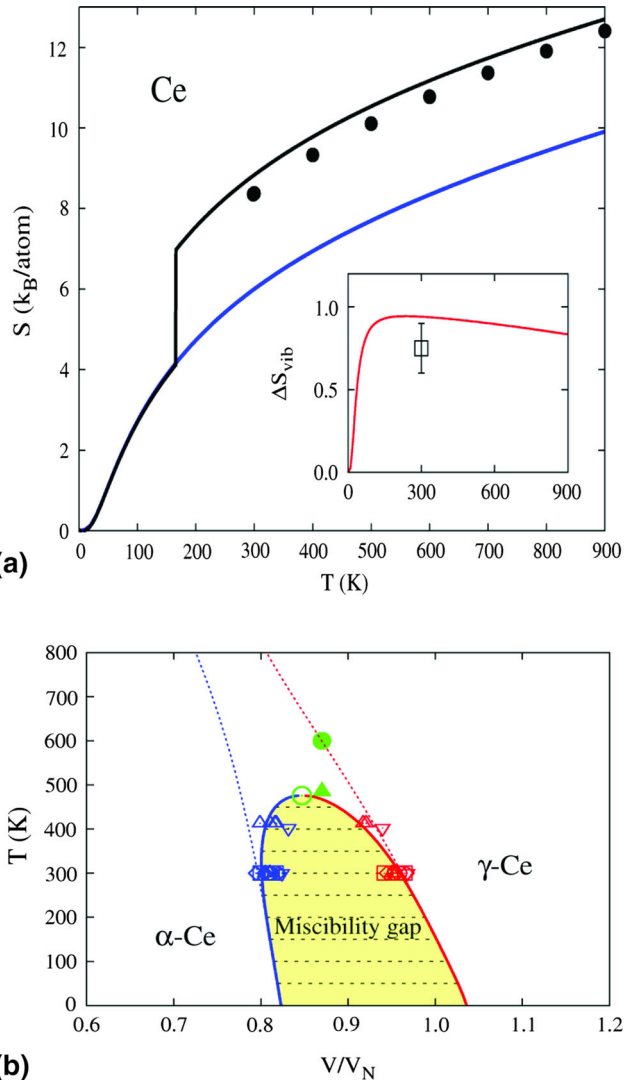

Fig. 2 (a) Total entropy, S, and vibrational entropy change, ΔS_{vib}, of Ce at 0 GPa with T (K) and (b) T–V phase diagram of Ce, with details in Ref. 46

'local-moment' mechanism[46] was corrected, and the critical point was predicted at $T_C = 546\,\text{K}$ and $P_C = 2.05\,\text{GPa}$, closer to the commonly accepted values than our previous predictions. The key is that the interactions between two configurations when they fluctuate is included in the thrid configuration.

The underlying physics of our 'itinerant-electron' magnetism model[48] closely resembles the Kondo-Anderson magnetic model as summarized by Kouwenhoven and Glazman.[49] At low temperatures, the Kondo-Anderson model states that impurity magnetic moment and one conduction electron moment bind and form an overall nonmagnetic configuration, while at high temperatures, the binding is broken resulting in a magnetic entropy of approximately $k_B \ln 2$. In our itinerant-magnetism model for the Ce transition, the nonmagnetic is the occupied

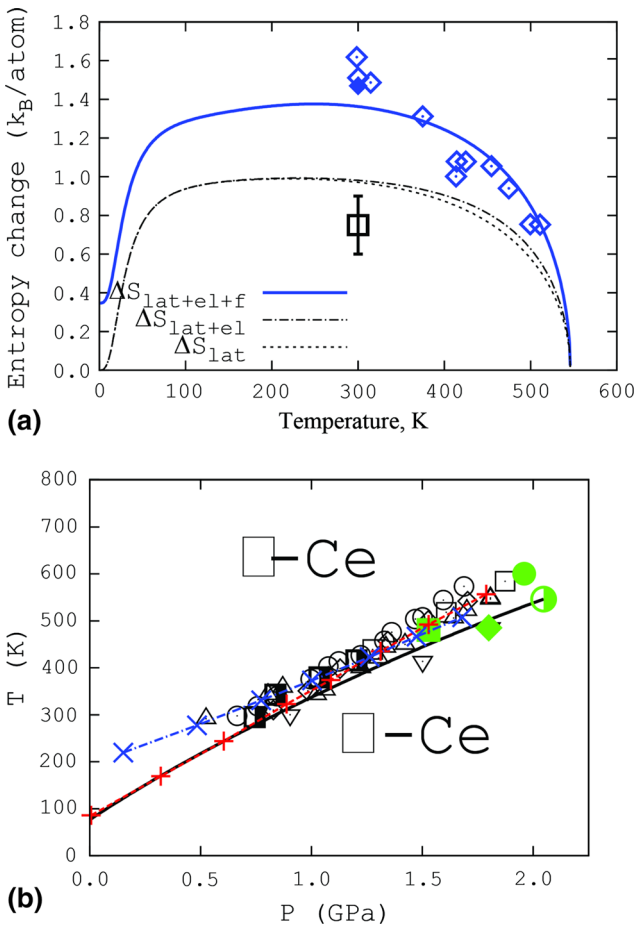

Fig. 3 (a) Predicted entropy changes in terms of lattice vibration (lat), lattice vibration plus thermal electron (lat + el), and lattice vibration plus thermal electron and plus configuration coupling (lat + el + f) changes along the phase boundary, (b) Predicted T–P phase diagram, both in comparison with experimental data with details in Ref. 48

ground configuration and the magnetic configurations are empty at 0 K. At finite temperatures, our model has a magnetic entropy term as shown by Eq 7, slightly different from the simple Kondo-Anderson model. At high enough temperatures the mixture between the FM and AFM configurations results in a magnetic entropy of $\sim k_B \ln 2$ as shown by the populations of configurations in Fig. 4.

It should be noted that the changes of all physical properties diverge at the critical point as shown by Eq 25. For example, Fig. 5(a) plots the predicted T–V phase diagram of Ce with isobaric volume curves and available experimental data superimposed. It can be seen that $\frac{\partial V}{\partial T} \Rightarrow +\infty$ at the critical point marked by the green circle, and significant anomaly exists at pressures considerably away from the pressure at the critical point. Since V and T are not conjugate variables in the combined law of thermodynamics (see Eq 2),[11] the positive sign of $\frac{\partial V}{\partial T}$ is not

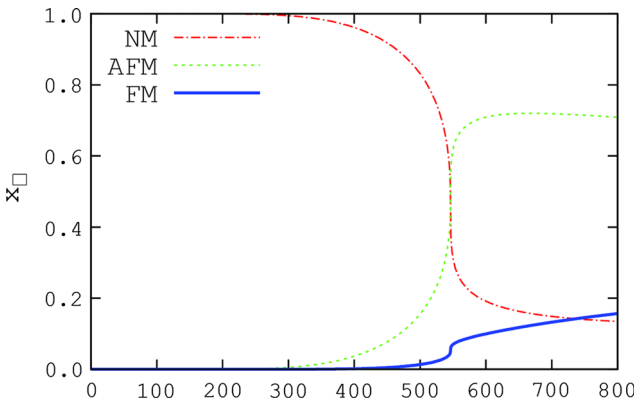

Fig. 4 Thermal populations, i.e. p^k, of the nonmagnetic (red dot-dashed), anti-ferromagnetic (green dashed), and ferromagnetic (blue solid) as a function of temperature at the critical pressure of 2.05 GPa from Ref. 48

thermodynamically guaranteed. It depends on the volumes of the metastable configurations.[50,51]

For example, the isobaric volume curves in the T–V phase diagram of Invar Fe_3Pt in Fig. 5(b) show $\frac{\partial V}{\partial T} \Rightarrow -\infty$ at the critical point marked by the green circle and $\frac{\partial V}{\partial T} < 0$ in a considerable temperature ranges away from the critical point. In this system, a supercell with 9 Fe and 3 Pt atoms was considered, resulting in 2^9=512 magnetic configurations with 37 of them being unique due to the symmetry. This negative thermal expansion or thermal contraction is because the metastable magnetic spin-flip configurations have smaller molar volumes than the FM configuration in Fe_3Pt. When the probability of the metastable magnetic spin-flip configurations increases with temperature due to their higher entropies than that of the FM configuration, the thermal expansion of the system, i.e. $\frac{\partial V}{\partial T}$, is the result of the competition between the positive thermal expansion of each configuration and the volume reduction due to the replacement of the FM configuration by the magnetic spin-flip configurations. When the latter is larger than the former, the thermal expansion of the system becomes negative. These anomalies can be generalized to a wide range of emergent behaviors for all physical properties of a system, when a system exhibits properties that its constituents do not possess such as negative thermal expansion in Fe_3Pt discussed above, with respect to composition and elastic, electric, magnetic fields, and their combinations with the present model as the theoretical foundation.[14,44,45,51]

In both Ce and Fe_3Pt cases, the configurations in the $k \in \{1, \ldots, m\}$ scale are various magnetic configurations with two sets of sub-configurations, i.e. thermal electronic and vibrational configurations, in the $l_1 \in \{1, \ldots, n_1\}$ and $l_2 \in \{1, \ldots, n_2\}$ scales. Based on the discussions in section 3, it is possible to construct two new sets of thermal electronic and vibrational configurations averaged across

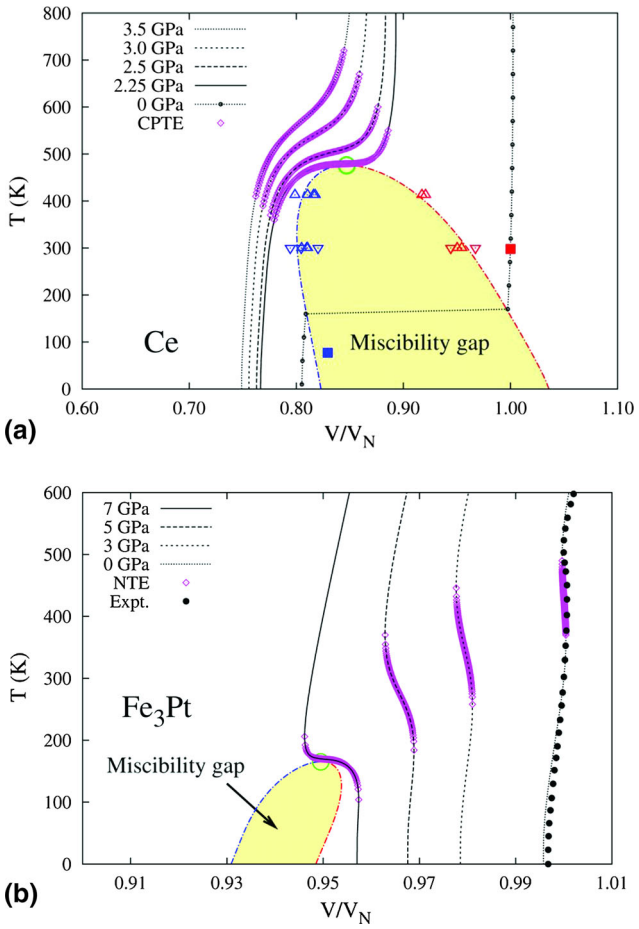

Fig. 5 Predicted temperature–volume phase diagrams with the miscibility gap (yellow shaded area) and critical point (green circle) marked,[8] (a) cerium and (b) Fe_3P. Additional isobaric volumes are plotted for several pressures with available experimental data superimposed

various magnetic configurations so that the thermal electronic and vibrational properties of the system can be predicted. The corresponding results are being investigated and will be published separately.

Let us consider the Al-Zn binary system with its phase diagram under ambient pressure shown in Fig. 6(a) calculated from the CALPHAD database in the literature[52] with a miscibility gap in the fcc phase. When the Gibbs energy is plotted with respect to the composition of Zn in Fig. 6(b), its curvature, i.e. the chemical potential derivative with respect to composition, changes sign in accordance with the stability criterion that the derivative of a potential with respect to its conjugate molar quantity changes sign at the limit of stability.[11] However, the plot of the internal energy with respect to entropy in Fig. 6(c) does not change its curvature as it should when crossing the stability boundary based on Eq 24. This indicates that the present CALPHAD modeling of critical phenomena needs to be further improved with multiple configurations as discussed above.[45]

7 Unresolved Issues in ABO_3 Perovskites

ABO_3 perovskites represent a group of ferroelectric materials that directly convert electrical energy to mechanical energy or vice versa. Many of them experience ferroelectric-paraelectric (FE-PE) phase transitions as a function of temperature or electric field. As an insulator, lead titanate ($PbTiO_3$, PTO) is a benchmark ferroelectric material. The phase transition between its two known perovskite structures, i.e. the ferroelectric tetragonal phase and the para-electric cubic phase,[53] occurs at about 763 K at ambient pressure and at room temperature at about 12 GPa[54,55] and has been considered as a classical example to understand structural and ferroelectric phase transitions in perovskites.[44,54,56–58]

The ferroelectricity in the tetragonal $PbTiO_3$ phase is due to the displacement of Ti atoms away from the center position in the tetragonal structure, resulted in spontaneous electric polarization. While the FE-PE phase transition is regarded as the typical displacive transition associated with softening of the relevant phonon modes, a certain degree of order–disorder mechanism has been considered in the literature associated with the orientation change of local distortions.[59,60] The direct calculation of the free energy of the para-electric cubic $PbTiO_3$ phase in terms of Eq 28 is not possible because its vibrational free energy cannot be evaluated due to its instability at zero K and ambient pressure. On the other hand, x-ray absorption fine-structure (XAFS) measurements by Sicron et al.[59] showed that the Ti atoms are displaced relative to the oxygen octahedra cage center both below and above the FE-PE phase transition temperature.

Through AIMD simulations shown in Fig. 7, Fang et al.[44] observed that the amount of tetragonal configuration decreases with the increase of temperature and reaches a plateau slightly below 50% above the FE-PE transition temperature in the cubic $PbTiO_3$ phase region with this transition temperature defined by the x-ray diffractions with lower time and spatial resolutions than those of XAFS (Fig. 7a).[54] Figure 7(b) also shows that about 80% of the tetragonal configurations in the cubic phase region are polarized though the over-all polarization is almost zero.[44] The other half of the Ti atoms in the cubic configuration are on transition from one to another polarization directions at any moment of time.[45] This observation confirms our theory as discussed in the previous section for Invar Fe_3Pt and anti-Invar Ce, i.e. high-temperature structures are dynamic averages of low-temperature configurations.

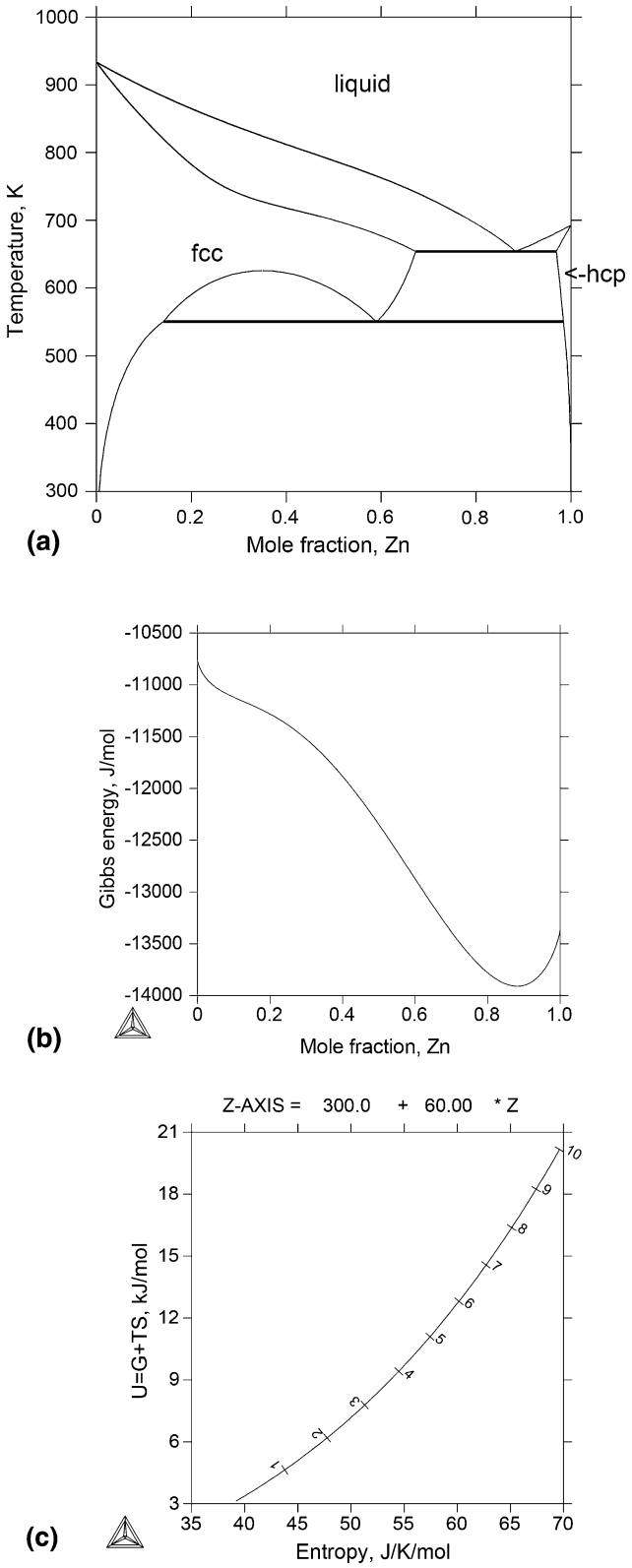

Fig. 6 (a) Calculated temperature-composition phase diagram of Al-Zn under ambient pressure from the CALPHAD database by Mey [52]; (b) Gibbs energy of the fcc phase as a function of Zn content at 373 K shown that the curvature of the curve, i.e. $\frac{\partial^2 G}{\partial (x_{Zn})^2}$, changes sign with respect to Zn content with the region of negative curvature being unstable; (c) Internal energy of the fcc phase as a function of entropy at mole fraction of Zn equal to 0.35 shown that $\frac{\partial^2 U}{\partial S^2}$ does not change sign with respect to entropy. The numbers on the curve are used to calculate the temperature in Kelvin using the function shown above the figure

In order to be able to predict the phonon properties of insulating polar materials with LO-TO splitting (splitting between longitudinal and transverse optical phonon frequencies)[61] using the direct (or supercell, small displacement, frozen phonon) method, we developed an approach that combines the accurate force constants calculated by the direct method in real space and the long-range dipole–dipole interactions calculated by linear response theory in reciprocal space.[62,63] To address the imaginary phonon modes predicted by first-principles calculations for ideal cubic ABO_3 perovskites, we used a pseudo-cubic supercell, i.e. with the shape of the supercell being cubic, but allowing the internal atomic positions fully relaxed, to successfully predict the experimentally observed phonon dispersion curves of $SrTiO_3$[64] and $PbTiO_3$,[65] but this approach can only predict first-order transition and cannot predict the second-order transition and the critical point.

Therefore, the challenge remains how to define the low-temperature configurations for ABO_3 in general and $PbTiO_3$ in particular. For Ce and Fe_3Pt, consideration of magnetic configurations with spins in two directions was sufficient. For $PbTiO_3$, it seems that the polarizations in six directions are needed based on the results from AIMD simulations,[44,45] resulted in a huge number of configurations even for a 40 atom supercell with 8 Ti atoms, i.e. $6^8 = 1,679,616$ configurations. It is self-evident that a new strategy is needed to discover those low energy, relevant configurations, and we are actively working on this topic.

8 Information Entropy and Internal Processes

Szilard[66,67] was probably the first to make a link between entropy and information when he tackled the famous Maxwell's demon through thought experiments. He rigorously demonstrated that a "biological phenomenon" of a nonliving device generates the same quantity of entropy required by thermodynamics, a critical link in the integration of physical and cognitive concepts that later became the foundation of information theory and a key idea in complex systems. In investigating the mathematical solution to communication and message transmission

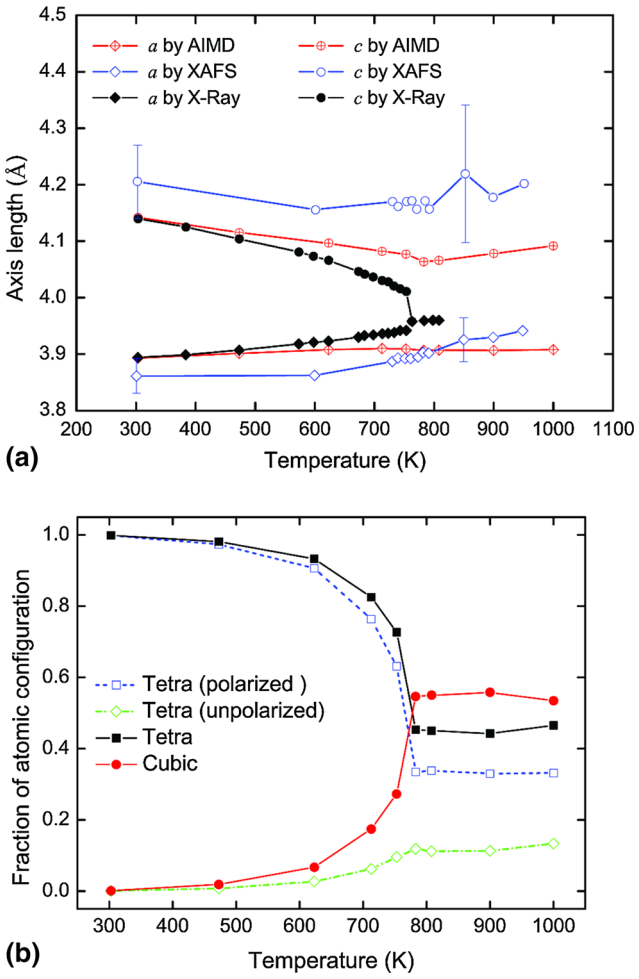

Fig. 7 (a) Temperature dependence of the lattice parameters *a, c* of $PbTiO_3$ unit cell, crossed symbols from AIMD simulations,[44] the open symbols from the XAFS measurements[59,86] and the closed symbols are from the x-ray diffraction,[54] (b) Fractions of the tetragonal (closed squares) with and without polarization and cubic (closed circles) and configurations as a function of temperature from the AIMD simulations[44]

problems, Shannon[4,68] proposed the concept of information entropy as the measure of the amount of information that is *missing* before reception or before communication is achieved and defined the information entropy as a macrostate (a source) with the number of possible microstates (ensembles of possible messages) that could be sent by that source. Thus, information in the communication begins with a set of messages, each with a probability, and the average information content per message is defined in analogy with Eq 7.

Brillouin extensively studied the relations between thermodynamics and information and suggested that information can be quantified using a system's entropy.[69–73] He noted that entropy itself measures the lack of information about the actual structure of a system and proposed that information corresponds to a negative term in the final entropy of a physical system as follows[70]

$$S_{\text{final}} = S_{\text{initial}} - I \qquad \text{(Eq 29)}$$

where S_{initial} and S_{final} are the initial and final entropies of the system, and I the information of the system. Brillouin's idea of dealing with information and physical entropy on an equal basis has been widely accepted in the community.[74] The exchange between energy and information was further elaborated by Landauer[75,76] who perceived that a logically irreversible process reduces the degrees of freedom of the system, thus entropy, and therefore must dissipate energy into the environment, hence erasing information in memory entails entropy increase in the environment. This is commonly referred to as Landauer's erasure principle, also investigated theoretically by Bennett[77] and more recently verified experimentally.[78,79]

Let us use the IP discussed in the present paper to understand the concept of information and its generation or loss. This IP may consume some masses/nutrients $\left(dN_i^n\right)$, generate some output masses/wastes $\left(dN_j^w\right)$ and heat $\left(d_{\text{ip}}Q\right)$, and re-organize its configurations to produce certain amount of information $\left(d_{\text{ip}}I\right)$, resulting in the entropy production with a similar form as Eq 1

$$d_{\text{ip}}S = \frac{d_{\text{ip}}Q}{T} - \sum S_i^n dN_i^n + \sum S_j^w dN_j^w - d_{\text{ip}}I \qquad \text{(Eq 30)}$$

where S_i^n and S_j^w are the entropies of nutrient i and waste j, respectively. Let us study several thought experiments of spontaneous IP, i.e. $d_{\text{ip}}S > 0$:

a. $dN_i^n = dN_j^w = 0$, the IP behaves like a closed system (i.e., involving no nutrient consumption and no waste generation)

   a.1. $d_{\text{ip}}I > 0$, the IP produces more information, and the sub-system must have $d_{\text{ip}}Q > Td_{\text{ip}}I > 0$, i.e. the IP must generate heat to be dissipated out to its surroundings, in accordance with the Landauer's erasure principle. The more information is reflected by the more distinct configurations, such as formation of crystal from its liquid and data writing;[68,80–82]

   a.2. $d_{\text{ip}}I < 0$, with information loss and $d_{\text{ip}}Q > Td_{\text{ip}}I$. Since $Td_{\text{ip}}I$ is negative, $d_{\text{ip}}Q$ could be either positive or negative.

      a.2.1. $d_{\text{ip}}Q < 0$: the IP absorbs heat from the outside of the sub-system, and the less information is reflected by the resulted fewer distinct configurations, such as

melting of crystal into its liquid and the data erasing;

a.2.2. $d_{\mathrm{ip}}Q > 0$: the IP produces more heat, resulting in self-destruction, such as fire.

b. $dN_i^n > 0$ and $dN_j^w > 0$, the IP behaves like an open system (i.e., involving nutrient consumption and waste generation). By definition, neither dN_i^n nor dN_j^w can be negative as their signs are pre-determined by the signs in front of them in Eq 30.

b.1. $-\sum S_i^n dN_i^n + \sum S_j^w dN_j^w = dS^{nw} > 0$, more waste entropy than nutrient entropy, and $d_{\mathrm{ip}}Q > Td_{\mathrm{ip}}I - TdS^{nw}$ for a spontaneous IP

b.1.1. $d_{\mathrm{ip}}I > 0$: the IP either must produce heat if $Td_{\mathrm{ip}}I > TdS^{nw}$ as in a.1 or produce/absorb heat which importantly indicates that the IP may produce more information through intensive metabolism without generating heat or with reduced heat generation;

b.1.2. $d_{\mathrm{ip}}I < 0$: the IP can either absorb or produce heat as in the case in a.2.

b.2. $-\sum S_i^n dN_i^n + \sum S_j^w dN_j^w = dS^{nw} < 0$, lower waste entropy than nutrient entropy, and $d_{\mathrm{ip}}Q > Td_{\mathrm{ip}}I - TdS^{nw}$ for a spontaneous IP.

b.2.1. $d_{\mathrm{ip}}I > 0$: the IP must produce heat as in a.1, but with the amount being $Td_{\mathrm{ip}}I - TdS^{nw}$, larger than $Td_{\mathrm{ip}}I$ by $-TdS^{nw}$, such as the growth of young organisms;

b.2.2. $d_{\mathrm{ip}}I < 0$: the IP must produce heat if $Td_{\mathrm{ip}}I > TdS^{nw}$ and may produce/absorb heat if $Td_{\mathrm{ip}}I < TdS^{nw}$ as in the case in a.2, noting that $dS^{nw} < 0$.

b.3. $-\sum S_i^n dN_i^n + \sum S_j^w dN_j^w = dS^{nw} = 0$, a steady state in terms of balanced entropy between nutrients and wastes. This case is similar to those in a.1 and in a.2, but with a constant of mass flow in and out of the spontaneous IP.

From Eq 30, one can further write the information change for an irreversible process ($d_{\mathrm{ip}}S > 0$) as follows

$$d_{\mathrm{ip}}I < \frac{d_{\mathrm{ip}}Q}{T} - \sum S_i^n dN_i^n + \sum S_j^w dN_j^w \qquad \text{(Eq 31)}$$

which gives the upbound of information that can be produced by an internal process. It can be seen that the information generation (loss) can be increased (decreases) with higher heat production, lower entropy of nutrient inputs, and higher entropy of waste outputs. It should be pointed out that even though the entropy change due to internal processes is only part of total entropy change of the system, the information change of the system is fully dictated by the internal processes in the system which are regulated by the heat and mass exchanges between the system and its surroundings that control the available nutrients for internal processes, as shown by Eq 1 and 30.

The total information change of a system would be the sum of individual internal processes. Following the discussions by Shannon[4,68] and Brillouin[69–73] we can rewrite Eq 8 and 9 as follows

$$S = -I^k + \sum_{k=1}^{m} p^k S^k \qquad \text{(Eq 32)}$$

$$S^k = -I^{l|k} + \sum_{l=1}^{n} p^{l|k} S^{l|k} \qquad \text{(Eq 33)}$$

$$I^k = -S^{\mathrm{conf}} = k_B \sum_{k=1}^{m} p^k \ln p^k \qquad \text{(Eq 34)}$$

$$I^{l|k} = k_B \sum_{l=1}^{n} p^{l|k} \ln p^{l|k} \qquad \text{(Eq 35)}$$

where I^k and $I^{l|k}$ denote the information in the system level, i.e., scale $k \in \{1, \ldots, m\}$, and the sub-scale level of $l \in \{1, \ldots, n\}$, respectively. The sub-scale information affects the system level information through its contribution to the probability p^k as shown by F^k in Eq 21.

As all spontaneous internal processes produce entropy, one may tend to think that the information of the universe has been decreasing from the beginning of time if the beginning of time could be defined such as by the Big Bang though certain sub-systems may experience an increase of their information as discussed in the thought experiments. As the sub-systems are brought across their limits of stability through the interactions with their surroundings, self-organized structures result. This is what discussed by Kondepudi and Prigogine,[15] that instability in a system enables the generation of dissipated structures, thus more distinct configurations, as also demonstrated in three examples in section 6. Therefore, the fundamentals of thermodynamics and information discussed in the present paper provide a framwwork for investigations of complex systems such as nano devices,[83] quantum computing,[82,84] and ecosystems.[6,85]

9 Summary

The fundamentals of entropy are discussed in this paper emphasizing its statistic nature, configurations, and information in comparable time and space scales. It is pointed out that the entropies of individual configurations play an essential role in determining their statistic probabilities and thus the configurational entropy and information of the

system. While a critical point is usually viewed as the divergence of entropy change with respect to temperature when the critical point is approached from a homogeneous system, it can also be considered as a mixture of competing configurations with the metastable configurations having higher entropies than the stable one. The importance of including key configurations containing features of interfaces among configurations is discussed in cerium. It is anticipated that the present model has the potential to be applied to a wide range of emergent behaviors and information change in small and large systems.

Acknowledgments ZKL is grateful for financial supports from many funding agencies in the United States as listed in the cited references, including the National Science Foundation (NSF with the latest Grant 1825538), the Department of Energy (with the latest Grants being DE-FE0031553 and DE-NE0008757), Army Research Lab, Office of Naval Research (with the latest Grant N00014-17-1-2567), Wright Patterson AirForce Base, NASA Jet Propulsion Laboratory, and the National Institute of Standards and Technology, plus a range of national laboratories and companies that supported the NSF Center for Computational Materials Design, the LION clusters at the Pennsylvania State University, the resources of NERSC supported by the Office of Science of the U.S. Department of Energy under Contract No. DE-AC02-05CH11231, and the resources of XSEDE supported by NSF with Grant ACI-1053575. BL would like to acknowledge the partial financial support from the NSF Grant Number DMS-1713078. The authors thank Prof. Yi Wang at Penn State for stimulating discussions.

References

1. C. Kittel, *Introduction to Solid State Physics*, Wiley, New York, 2005
2. S.W. Hawking, Black Holes and Thermodynamics, *Phys. Rev. D*, 1976, **13**, p 191-197
3. F. Ross, S.W. Hawking, and G.T. Horowitz, Entropy, Area, and Black Hole Pairs, *Phys. Rev. D*, 1995, **51**, p 4302-4314
4. C.E. Shannon, A Mathematical Theory of Communication, *Bell Syst. Tech. J.*, 1948, **27**, p 623-656
5. S. Pavoine, S. Ollier, and D. Pontier, Measuring Diversity from Dissimilarities with Rao's Quadratic Entropy: Are Any Dissimilarities Suitable?, *Theor. Popul. Biol.*, 2005, **67**, p 231-239
6. J. Quijano and H. Lin, Entropy in the Critical Zone: A Comprehensive Review, *Entropy*, 2014, **16**, p 3482-3536
7. M.A. Busa and R.E.A. van Emmerik, Multiscale Entropy: A Tool for Understanding the Complexity of Postural Control, *J. Sport Heal. Sci.*, 2016, **5**, p 44-51
8. Z.K. Liu, Y. Wang, and S.L. Shang, Thermal Expansion Anomaly Regulated by Entropy, *Sci. Rep.*, 2014, **4**, p 7043
9. K.G. Wilson, The Renormalization Group: Critical Phenomena and the Kondo Problem, *Rev. Mod. Phys.*, 1975, **47**, p 773-840
10. A. Pelissetto and E. Vicari, Critical Phenomena and Renormalization-Group Theory, *Phys. Rep.-Rev. Sect. Phys. Lett.*, 2002, **368**, p 549-727
11. Z.K. Liu and Y. Wang, *Computational Thermodynamics of Materials*, Cambridge University Press, Cambridge, 2016
12. M. Hillert, *Phase Equilibria, Phase Diagrams and Phase Transformations: Their Thermodynamic Basis*, Cambridge University Press, Cambridge, 2008
13. J.W. Gibbs, *The Collected Works of J. Willard Gibbs: Vol. I, Thermodynamics*, Yale University Press, New Haven, 1948
14. Z.K. Liu, X.Y. Li, and Q.M. Zhang, Maximizing the Number of Coexisting Phases Near Invariant Critical Points for Giant Electrocaloric and Electromechanical Responses in Ferroelectrics, *Appl. Phys. Lett.*, 2012, **101**, p 82904
15. D. Kondepudi and I. Prigogine, *Modern Thermodynamics: From Heat Engines to Dissipative Structures*, Wiley, New York, 1998
16. J.W. Gibbs, *The Collected Works of J. Willard Gibbs: Vol. II, Statistic Mechanics*, Yale University Press, New Haven, 1948
17. S.M. Ross, *A First Course in Probability*, Pearson, London, 2012
18. L.D. Landau and E.M. Lifshitz, *Statistical Physics*, Pergamon Press Ltd., New York, 1980
19. M. Asta, R. McCormack, and D. de Fontaine, Theoretical Study of Alloy Stability in the Cd-Mg System, *Phys. Rev. B*, 1993, **48**, p 748
20. Y. Wang, S.L. Shang, H. Zhang, L.Q. Chen, and Z.K. Liu, Thermodynamic Fluctuations in Magnetic States: Fe3Pt as a Prototype, *Philos. Mag. Lett.*, 2010, **90**, p 851-859
21. H.L. Lukas, S.G. Fries, and B. Sundman, *Computational Thermodynamics: The CALPHAD Method*, Vol 131, Cambridge University Press, Cambridge, 2007
22. L. Kaufman and H. Bernstein, *Computer Calculation of Phase Diagram*, Academic Press Inc., New York, 1970
23. W. Kohn and L.J. Sham, Self-Consisten Equations Including Exchange and Correlation Effects, *Phys. Rev.*, 1965, **140**, p A1133-A1138
24. G. Kresse, J. Furthmüller. Vienna Ab-initio Simulation Package (VASP). https://www.vasp.at. Accessed 13 Jan 2019
25. Quantum Espresso. http://www.quantum-espresso.org/. Accessed 13 Jan 2019
26. The Extreme Science and Engineering Discovery Environment (XSEDE). https://www.xsede.org/. Accessed 13 Jan 2019
27. National Energy Research Scientific Computing Center (NERSC). http://www.nersc.gov/. Accessed 13 Jan 2019
28. Materials Project. http://materialsproject.org/. Accessed 13 Jan 2019
29. OQMD: An Open Quantum Materials Database. http://oqmd.org. Accessed 13 Jan 2019
30. AFLOW: Automatic Flow for Materials Discovery. http://www.aflowlib.org. Accessed 13 Jan 2019
31. A. van de Walle and G. Ceder, The Effect of Lattice Vibrations on Substitutional Alloy Thermodynamics, *Rev. Mod. Phys.*, 2002, **74**, p 11-45
32. Y. Wang, Z.K. Liu, and L.Q. Chen, Thermodynamic Properties of Al, Ni, NiAl, and Ni3Al from First-Principles Calculations, *Acta Mater.*, 2004, **52**, p 2665-2671
33. S.L. Shang, Y. Wang, D. Kim, and Z.K. Liu, First-Principles Thermodynamics from Phonon and Debye Model: Application to Ni and Ni_3Al, *Comput. Mater. Sci.*, 2010, **47**, p 1040-1048
34. X.L. Liu, B.K. Vanleeuwen, S.L. Shang, Y. Du, and Z.K. Liu, On the Scaling Factor in Debye–Grüneisen Model: A Case Study of the Mg-Zn Binary System, *Comput. Mater. Sci.*, 2015, **98**, p 34-41
35. S.L. Shang, Y. Wang, and Z.K. Liu, First-Principles Elastic Constants of α- and θ-Al_2O_3, *Appl. Phys. Lett.*, 2007, **90**, p 101909
36. S.L. Shang, H. Zhang, Y. Wang, and Z.K. Liu, Temperature-Dependent Elastic Stiffness Constants of Alpha- and Theta-Al_2O_3 from First-Principles Calculations, *J. Phys. Condens. Matter*, 2010, **22**, p 375403
37. Y. Wang, J.J. Wang, H. Zhang, V.R. Manga, S.L. Shang, L.Q. Chen, and Z.K. Liu, A First-Principles Approach to Finite Temperature Elastic Constants, *J. Phys. Condens. Matter*, 2010, **22**, p 225404

38. J.M. Sanchez, Cluster Expansion and the Configurational Energy of Alloys, *Phys. Rev. B: Condens. Matter*, 1993, **48**, p R14013-R14015
39. A. van de Walle, M. Asta, and G. Ceder, The Alloy Theoretic Automated Toolkit: A User Guide, *CALPHAD*, 2002, **26**, p 539-553
40. A. Zunger, S.H. Wei, L.G. Ferreira, and J.E. Bernard, Special Quasirandom Structures, *Phys. Rev. Lett.*, 1990, **65**, p 353-356
41. C. Jiang, C. Wolverton, J. Sofo, L.Q. Chen, and Z.K. Liu, First-Principles Study of Binary bcc Alloys Using Special Quasirandom Structures, *Phys. Rev. B*, 2004, **69**, p 214202
42. A. van de Walle, P. Tiwary, M. de Jong, D.L. Olmsted, M. Asta, A. Dick, D. Shin, Y. Wang, L.-Q. Chen, and Z.K. Liu, Efficient Stochastic Generation of Special Quasirandom Structures, *CALPHAD*, 2013, **42**, p 13-18
43. R. Car and M. Parrinello, Unified Approach for Molecular-Dynamics and Density-Functional Theory, *Phys. Rev. Lett.*, 1985, **55**, p 2471-2474
44. H.Z. Fang, Y. Wang, S.L. Shang, and Z.K. Liu, Nature of Ferroelectric-Paraelectric Phase Transition and Origin of Negative Thermal Expansion in $PbTiO_3$, *Phys. Rev. B*, 2015, **91**, p 24104
45. Z.K. Liu, Ocean of Data: Integrating First-Principles Calculations and CALPHAD Modeling with Machine Learning, *J. Phase Equilib. Diffus.*, 2018, **39**, p 635-649
46. Y. Wang, L.G. Hector, H. Zhang, S.L. Shang, L.Q. Chen, and Z.K. Liu, Thermodynamics of the Ce Gamma-Alpha Transition: Density-Functional Study, *Phys. Rev. B*, 2008, **78**, p 104113
47. G. Kresse, J. Furthmuller, J. Furthmüller, J. Furthmueller, J. Furthmuller, and J. Furthmüller, Efficient Iterative Schemes for Ab Initio Total-Energy Calculations Using a Plane-Wave Basis Set, *Phys. Rev. B*, 1996, **54**, p 11169
48. Y. Wang, L.G. Hector, H. Zhang, S.L. Shang, L.Q. Chen, and Z.K. Liu, A Thermodynamic Framework for a System with Itinerant-Electron Magnetism, *J. Phys. Condens. Matter*, 2009, **21**, p 326003
49. L. Kouwenhoven and L. Glazman, Revival of the Kondo Effect, *Phys. World*, 2001, **14**, p 33-38
50. Z.K. Liu, Y. Wang, and S.-L. Shang, Origin of Negative Thermal Expansion Phenomenon in Solids, *Scr. Mater.*, 2011, **66**, p 130
51. Z.K. Liu, S.L. Shang, and Y. Wang, Fundamentals of Thermal Expansion and Thermal Contraction, *Materials (Basel)*, 2017, **10**, p 410
52. S.A. Mey, Reevaluation of the Al-Zn System, *Z. Met.*, 1993, **84**, p 451-455
53. Z.K. Liu, Z.G. Mei, Y. Wang, and S.L. Shang, Nature of Ferroelectric–Paraelectric Transition, *Philos. Mag. Lett.*, 2012, **92**, p 399-407
54. G. Shirane and S. Hoshino, On the Phase Transition in Lead Titanate, *J. Phys. Soc. Jpn.*, 1951, **6**, p 265
55. S.G. Jabarov, D.P. Kozlenko, S.E. Kichanov, A.V. Belushkin, B.N. Savenko, R.Z. Mextieva, and C. Lathe, High Pressure Effect on the Ferroelectric-Paraelectric Transition in $PbTiO_3$, *Phys. Solid State*, 2011, **53**, p 2300-2304
56. D. Damjanovic, Ferroelectric, Dielectric and Piezoelectric Properties of Ferroelectric Thin Films and Ceramics, *Rep. Prog. Phys.*, 1998, **61**, p 1267-1324
57. J. Chen, X. Xing, C. Sun, P. Hu, R. Yu, X. Wang, and L. Li, Zero Thermal Expansion in $PbTiO_3$-Based Perovskites, *J. Am. Chem. Soc.*, 2008, **130**, p 1144-1145
58. P.-E. Janolin, P. Bouvier, J. Kreisel, P.A. Thomas, I.A. Kornev, L. Bellaiche, W. Crichton, M. Hanfland, and B. Dkhil, High-Pressure $PbTiO_3$: An Investigation by Raman and X-Ray Scattering up to 63 GPa, *Phys. Rev. Lett.*, 2008, **101**, p 237601
59. N. Sicron, B. Ravel, Y. Yacoby, E.A. Stern, F. Dogan, and J.J. Rehr, Nature of the Ferroelectric Phase-Transition in $PbTiO_3$, *Phys. Rev. B*, 1994, **50**, p 13168-13180
60. K. Sato, T. Miyanaga, S. Ikeda, and D. Diop, XAFS Study of Local Structure Change in Perovskite Titanates, *Phys. Scr.*, 2005, **2005**, p 359
61. W. Cochran and R.A. Cowley, Dielectric Constants and Lattice Vibrations, *J. Phys. Chem. Solids*, 1962, **23**, p 447-450
62. Y. Wang, J.J. Wang, W.Y. Wang, Z.G. Mei, S.L. Shang, L.Q. Chen, and Z.K. Liu, A Mixed-Space Approach to First-Principles Calculations of Phonon Frequencies for Polar Materials, *J. Phys.-Condens. Matter*, 2010, **22**, p 202201
63. Y. Wang, S.L. Shang, H. Fang, Z.K. Liu, and L.Q. Chen, First-Principles Calculations of Lattice Dynamics and Thermal Properties of Polar Solids, *Comput. Mater.*, 2016, **2**, p 16006
64. Y. Wang, J.E. Saal, Z.G. Mei, P.P. Wu, J.J. Wang, S.L. Shang, Z.K. Liu, and L.Q. Chen, A First-Principles Scheme to Phonons of High Temperature Phase: No Imaginary Modes for Cubic $SrTiO_3$, *Appl. Phys. Lett.*, 2010, **97**, p 162907
65. M.J. Zhou, Y. Wang, Y. Ji, Z.K. Liu, L.Q. Chen, and C.-W. Nan, First-Principles Lattice Dynamics and Thermodynamic Properties of Pre-Perovskite $PbTiO_3$, *Acta Mater*, 2019, **171**, p 146-153
66. L. Szilard, Uber die Entropieverminderung in einem thermodynamischen System bei Eingriffen intelligenter Wesen, *Z. Phys.*, 1929, **53**, p 840-856
67. L. Szilard, On the Decrease of Entropy in a Thermodynamic System by the Intervention of Intelligent Beings, *Behav. Sci.*, 1964, **9**, p 301-310
68. C.E. Shannon, Prediction and Entropy of Printed English, *Bell Syst. Tech. J.*, 1951, **30**, p 50-64
69. L. Brillouin, Physical Entropy and Information. II, *J. Appl. Phys.*, 1951, **22**, p 338-343
70. L. Brillouin, The Negentropy Principle of Information, *J. Appl. Phys.*, 1953, **24**, p 1152-1163
71. L. Brillouin, Information Theory and Its Applications to Fundamental Problems in Physics, *Nature*, 1959, **183**, p 501-502
72. L. Brillouin, Thermodynamics, Statistics, and Information, *Am. J. Phys.*, 1961, **29**, p 318-328
73. L. Brillouin, *Science and Information Theory*, Academic Press, New York, 1962
74. K. Maruyama, F. Nori, and V. Vedral, Colloquium: The Physics of Maxwell's Demon and Information, *Rev. Mod. Phys.*, 2009, **81**, p 1-23
75. R. Landauer, Irreversibility and Heat Generation in the Computing Process, *IBM J. Res. Dev.*, 1961, **5**, p 183-191
76. R. Landauer, Dissipation and Noise Immunity in Computation and Communication, *Nature*, 1988, **335**, p 779-784
77. C.H. Bennett, The Thermodynamics of Computation—A Review, *Int. J. Theor. Phys.*, 1982, **21**, p 905-940
78. S. Toyabe, T. Sagawa, M. Ueda, E. Muneyuki, and M. Sano, Experimental Demonstration of Information-to-Energy Conversion and Validation of the Generalized Jarzynski Equality, *Nat. Phys.*, 2010, **6**, p 988-992
79. A. Bérut, A. Arakelyan, A. Petrosyan, S. Ciliberto, R. Dillenschneider, and E. Lutz, Experimental Verification of Landauer's Principle Linking Information and Thermodynamics, *Nature*, 2012, **483**, p 187-189
80. L. Brillouin, Negentropy and Information in Telecommunications, Writing, and Reading, *J. Appl. Phys.*, 1954, **25**, p 595-599
81. U. Seifert, Stochastic Thermodynamics, Fluctuation Theorems and Molecular Machines, *Rep. Prog. Phys.*, 2012, **75**, p 126001
82. P. Strasberg, G. Schaller, T. Brandes, and M. Esposito, Quantum and Information Thermodynamics: A Unifying Framework Based on Repeated Interactions, *Phys. Rev. X*, 2017, **7**, p 021003

83. E. Pop, Energy Dissipation and Transport in Nanoscale Devices, *Nano Res*, 2010, **3**, p 147-169
84. S. Vinjanampathy and J. Anders, Quantum Thermodynamics, *Contemp. Phys.*, 2016, **57**, p 545-579
85. S.E. Jørgensen, *A New Ecology: Systems Perspective*, Elsevier, Amsterdam, 2007
86. B. Ravel, N. Slcron, Y. Yacoby, E.A. Stern, F. Dogan, and J.J. Rehr, Order-Disorder Behavior in the Phase Transition of $PbTiO_3$, *Ferroelectrics*, 1995, **164**, p 265-277